Electron-Temperature Evolution in Expanding Ultracold Neutral Plasmas

P. Gupta, S. Laha, C. E. Simien, H. Gao, J. Castro, and T. C. Killian

Department of Physics and Astronomy, Rice University, Houston, Texas 77005, USA

T. Pohl

ITAMP, Harvard-Smithsonian Center for Astrophysics, 60 Garden Street, Cambridge, Massachusetts 02138, USA

We have used the free expansion of ultracold neutral plasmas as a time-resolved probe of electron temperature. A combination of experimental measurements of the ion expansion velocity and numerical simulations characterize the crossover from an elastic-collision regime at low initial Γ_e, which is dominated by adiabatic cooling of the electrons, to the regime of high Γ_e in which inelastic processes drastically heat the electrons. We identify the time scales and relative contributions of various processes, and we experimentally show the importance of radiative decay and disorder-induced electron heating for the first time in ultracold neutral plasmas.

Ultracold neutral plasmas (UNPs) [1,2] occupy an exotic regime of plasma physics in which electron and ion temperatures are orders of magnitude colder than in conventional neutral plasmas. The electron temperature in these systems evolves under the influence of many factors, which can occur on very different time scales, such as disorder-induced heating [3], three-body recombination [4,5], and adiabatic cooling [6,7]. The relative importance of the various effects depends critically upon initial conditions, and this has complicated the experimental study of the electron temperature [8–12] and leads to much theoretical debate [3,6,7,13,14]. We present here detailed experimental measurements and numerical simulations that untangle the time scales and contributions of the various competing effects and characterize the transition from elastic-collision-dominated to inelastic-collision-dominated behavior.

UNPs are of fundamental interest because they can be in or near the strongly coupled regime, which is characterized by the existence of spatial correlations between particles and a Coulomb coupling parameter $\Gamma = e^2/(4\pi\varepsilon_0 a k_B T) > 1$, where T refers to the temperature of the particles and $a = (4\pi n/3)^{-1/3}$ is the Wigner-Seitz radius. Ions in UNPs equilibrate with $\Gamma_i \sim 3$ [10,15]. The initial electron temperature is under experimental control and can be set such that a naïve calculation of Γ_e suggests that electrons are also strongly coupled. However, electrons rapidly leave the strongly coupled regime due to various heating mechanisms [3,6,14] that are central to studies presented here.

To create a UNP, strontium atoms from a Zeeman-slowed beam are trapped and cooled in a magneto-optical trap operating on the $^1S_0$-$^1P_1$ atomic transition at 461 nm [16]. A 10 ns pulse from a dye laser then excites about 20% of the atoms just above the ionization threshold. The temperature of the resulting ions is initially a few milli-kelvin, which is similar to the temperature of the laser-cooled neutral atoms, but ions heat within 1 μs to about

1 K due to disorder-induced heating [15,17]. The initial electron kinetic energy (E_e) equals the difference between the energy of the ionizing photon and the ionization threshold. With a tunable pulsed-dye laser, $2E_e/3k_B$ can be set from 1–1000 K. Electrons thermalize locally within 100 ns and globally within 1 μs [6]. Simple equilibration would set the initial $T_e = 2E_e/3k_B$, but we will discuss processes that can change T_e.

The plasma density follows the profile of the neutral atom cloud. By adjusting the laser-cooling parameters and imaging the cloud in two perpendicular axes, we ensure that the plasma has a spherically symmetric Gaussian profile, $n(r) = n_0 e^{-r^2/2\sigma^2}$. Deviations from spherical symmetry, e.g., $(\sigma_x - \sigma_y)/\sigma_x$, are less than 5%. Typically, the initial n_0 is $\sim 10^{16}$ m^{-3} and $\sigma \sim 1$ mm. The plasma is quasineutral $(n_i \sim n_e)$ with the Debye length $\lambda_D = (\varepsilon_0 k_B T_e/n_e e^2)^{1/2} \ll \sigma$, where n_i and n_e refer to ion and electron density, respectively. UNPs are unconfined and expand into the surrounding vacuum, and quasineutrality is maintained during the expansion.

Electron-temperature evolution during expansion of UNPs has been studied using various techniques. Electron plasma oscillations [8] measured the average density in order to obtain the rms radial terminal velocity of the ions. This showed that essentially all the initial electron energy is converted to ion expansion energy. In addition, plasmas with lower E_e and higher n_0 (which would imply $\Gamma_e \gtrsim 1$ [18]) resulted in an anomalously fast expansion. Numerical simulations [6] reproduced these observations; however, the relationship between density and the electron plasma oscillation used in [8] has been called into question in subsequent work [12,19]. Reference [9] probed T_e by measuring the fraction of electrons escaping the plasma during a small electric field pulse and inferred that for 10 K $< 2E_e/3k_B <$ 300 K and $n_0 \sim 5 \times 10^{14}$ m^{-3}, electrons approach a narrow temperature range (20 K $< T_e <$ 40 K) about 5 μs after photo-

ionization. Spatially resolved fluorescence detection of the ions [10,11] in a cylindrical plasma measured expansion energies similar to what was observed in [8], but showed significant deviations from theoretical predictions that perhaps arose because of the lack of spherical symmetry. Tonks-Dattner modes, which have T_e-sensitive resonances, were recently observed in UNPs [12], and experimental measurements agreed with a model that assumed constant T_e over 40 μs of evolution. So the electron-temperature evolution in UNPs is obviously a complicated problem that remains unsettled.

The results presented here have several advantages over previous studies. We have a spherically symmetric plasma that allows the application of exact analytic results. Doppler broadening of the ion optical absorption spectrum [2] provides a calibrated, model-independent measure of the ion velocity and overall plasma expansion with excellent temporal resolution stretching from the phase of initial ion acceleration to the onset of terminal velocity. A combination of experiment and numerical simulation allows the contributions of various electron heating and cooling mechanisms to be separated as never before, and we find excellent agreement between experiment and theory with no adjustable parameters. We also present a systematic study of the full spectrum of dynamics observed in current UNP experiments.

For an experimental probe, a narrowband laser at 422 nm passing through the plasma and falling on a CCD camera measures the Doppler width of the Sr^+ $^2S_{1/2}$-$^2P_{1/2}$ absorption spectrum for the entire plasma. This can be related to $\sqrt{\langle(\mathbf{v} \cdot \hat{\mathbf{z}})^2\rangle} \equiv v_{i,\mathrm{rms}}$ as described in [2], where $\hat{\mathbf{z}}$ is the laser propagation direction, $\mathbf{v}$ is the total ion velocity including random thermal motion and expansion ($\mathbf{u}$), and the angled brackets refer to an average over the plasma density and velocity distribution. In a quasineutral Gaussian plasma such as a UNP, the electron temperature can be found from measurements of $v_{i,\mathrm{rms}}$ due to its sensitivity to $\mathbf{u}$ and the fact that the expansion acceleration,

$$\dot{\mathbf{u}} = -\frac{k_B(T_e + T_i)}{m_i}\frac{\nabla n}{n},\qquad(1)$$

arises from thermal pressure [6–8,20].

For high E_e and low n_0, which we denote as the "elastic-collisional regime" ($\Gamma_e < 0.1$ [18]), all collisional processes in a UNP are elastic, the plasma expands adiabatically, and electrons cool [21]. This leads to a self-similar expansion that preserves the Gaussian phase-space distributions and is described by an analytic solution of the Vlasov equations [6,7] that was originally derived for short-pulse laser experiments [20,22,23] and applied to UNPs in [6,7]. UNPs provide the first clean realization of this analytic solution, and this was shown experimentally in [24]. The Vlasov equations do not include a collision term, which is appropriate because such a term vanishes for a Maxwell-Boltzmann velocity distribution. So in this

sense, the expansion in the elastic-collisional regime can also be called "collisionless" [20].

In this regime, $v_{i,\mathrm{rms}}$ is given by [24]

$$v_{i,\mathrm{rms}} = \sqrt{\frac{k_B}{m_i\tau_{\exp}^2}[t^2(T_e + T_i) + \tau_{\exp}^2 T_i]}.\qquad(2)$$

The characteristic expansion time $\tau_{\exp}$ is given by $\tau_{\exp} = \sqrt{m_i\sigma(0)^2/k_B[T_e(0) + T_i(0)]}$, and the electron and ion temperatures follow

$$T_{e/i} = T_{e/i}(0)/(1 + t^2/\tau_{\exp}^2).\qquad(3)$$

Figure 1(a) shows the ion-velocity evolution for UNPs in the elastic-collisional regime. Fits using Eq. (2) take $T_{i/e}(0)$ as fit parameters, while $\sigma(0)$ is fixed to the value found from the images. For higher E_e in Fig. 1, the fit is excellent and the extracted values of $T_e(0)$ yield $2E_e/3k_B$ within experimental uncertainty, confirming that inelastic collisions are negligible in this regime. The underlying electron-temperature evolution is shown in Fig. 1(b). As expected, T_e drops due to adiabatic cooling because there is no significant electron heating.

For $2E_e/3k_B = 25$ K in Fig. 1, the fit $T_e(0) = 33$ K exceeds the expected value. This provides evidence that inelastic processes are modifying the electron temperature. Many processes are expected to contribute. Within tens of nanoseconds, disorder-induced heating (DIH) [3,25] increases electron kinetic energy by as much as several kelvin above E_e in the range of our initial conditions. DIH is the conversion of potential energy into kinetic as spatial correlations develop. Three-body recombination (TBR) [4] populates Rydberg levels bound by $\sim k_B T_e$ and heats the free electrons. Rydberg-electron collisions (REC) [4,6] can transfer Rydberg atoms to more deeply bound
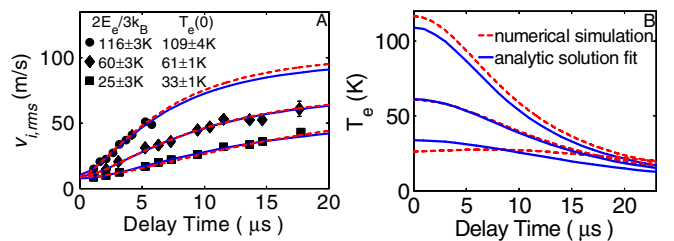

FIG. 1 (color online). Expansion velocity (a) and electron temperature (b) for low Γ_e showing little or no electron heating effects. (a) The initial peak densities and sizes are $n_0 = 3.5 \times 10^{15}$ m^{-3} and $\sigma(0) = 1$ mm. The self-similar analytic solution (dark solid line) provides an excellent fit of the data, with fitted $T_e(0)$ indicated in the legend. The full numerical simulation (dashed line) describes the data with no adjustable parameters. (b) Electron-temperature evolutions [Eq. (3)] are determined from parameters of the fits to $v_{i,\mathrm{rms}}$ or by numerical simulation. For $2E_e/3k_B = 25$ K, the analytic solution fit and numerical simulation for $T_e(t)$ deviate significantly, showing the importance of inelastic collision effects.

levels and heat electrons further, while radiative decay (RD) of the Rydberg atoms mitigates this heating effect. Direct cooling of electrons through equilibration with ions is negligibly slow for these experiments because of the large ion-electron mass difference [26].

To understand the interplay between these various effects, we performed numerical simulations, taking into account all relevant heating and cooling mechanisms. Our description is based on a particle-in-cell simulation of the ions and treats the electrons adiabatically as a fluid in a constantly changing equilibrium state [6,7]. DIH due to particle correlations is accounted for in the initial conditions of both plasma components [3,17], assuming a homogeneous T_e for the electrons and a homogeneous Γ_i for the ions. This treatment neglects the influence of correlations on later stages of the plasma dynamics, which may be a concern because UNP ions are strongly coupled [10,15], but [7] showed that the effects of ion-ion correlations on the expansion are negligible. Finally we use a Monte Carlo treatment to describe the formation of Rydberg atoms and their subsequent binding energy evolution, employing known expressions for the rates of TBR and REC [4] and RD [27]. The TBR rates [4] are well confirmed experimentally at high temperatures, but their low temperature validity has been questioned [28–30] as it ultimately must break down for $T_e \rightarrow 0$ due to its strong $\propto T_e^{-9/2}$ temperature divergence. By comparing experiments and calculations the present study indirectly tests TBR theory over a wide range of temperatures.

The numerical simulation reproduces the expansion dynamics in Fig. 1 with no adjustable parameters, and it shows that $2E_e/3k_B = 25$ K is on the border of the "inelastic collisional regime", which is defined here as initial $\Gamma_e > 0.1$ [18]. For this data set, $T_e(t)$ stays roughly constant over the observed evolution time and is not well described by the analytic solution [Eq. (3)]. Only TBR and REC processes must be included in the simulation to accurately describe the expansion.

Figure 2(a) displays characteristic plasma dynamics for lower initial electron energy and higher Γ_e that is in the inelastic collisional regime. The expansion is much faster than expected for elastic-collisional-regime dynamics with $T_e(0) = 2E_e/3k_B = 14$ K. Incorporating only TBR and REC in the simulation considerably overshoots the observed ion-velocity evolution because it overestimates electron heating. Inclusion of RD, which transfers Rydberg atoms to more deeply bound states without heating the plasma electrons, produces excellent agreement with experiment without adjustable parameters.

The analytic solution [Eq. (2)] provides a surprisingly accurate description of observed ion velocities, but the simulation shows [Fig. 2(b)] that the extracted $T_e(0)$ is only a phenomenological parameter. Physically, TBR and REC heat the electrons in the first ~ 5 μs, although it is mitigated by RD. The increasing T_e and decreasing density
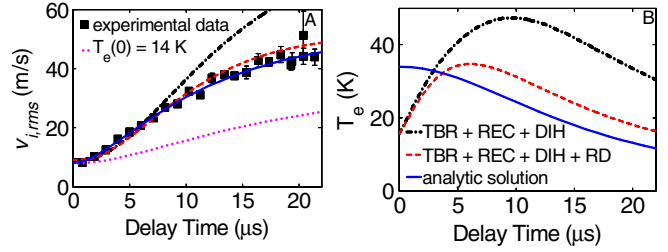

FIG. 2 (color online).   (a) Expansion velocity and (b) electron temperature for moderate initial $\Gamma_e = 0.2$ [$2E_e/3k_B = 14$ K, $\sigma(0) = 0.9$ mm, and $n_0(0) = 7 \times 10^{15}$ m^{-3}]. (a) A fit of the expansion to the analytic solution [Eq. (2), solid line] yields $T_e(0) = 34$ K, which reflects much faster expansion than expected for elastic-collisional dynamics with $2E_e/3k_B = 14$ K (dotted line). Only including TBR and REC in the simulation (dot-dashed line) overestimates the heating. Including RD as well (dashed line) brings theory into good agreement with experiment. Including DIH increases the initial electron temperature by about 3 K, but has little effect on the velocity fit. (b) The fit $T_e(0)$ approximately equals the maximum of the actual $T_e(t)$ obtained with simulation.

slow TBR, so that adiabatic cooling dominates at later times. The fit $T_e(0)$ gives a rough estimate of the maximum electron temperature, $T_{e,\text{max}}$.

Further decrease of E_e or increase in density pushes further into the inelastic collisional regime where a naïve calculation using $T_e = 2E_e/3k_B$ implies $\Gamma_e \gtrsim 1$. In this regime, fits using the analytic expansion expression fail to reproduce the data (Fig. 3). Simulations show that the approximation of a self-similar Gaussian expansion also becomes poor due to the large fraction of ions that undergo TBR and the higher rate for this process in the higher density central region of the plasma. The measured ion expansion velocity indicates the occurrence of extreme electron heating from $2E_e/3k_B = 4$ K. For this relatively high-density sample DIH makes a significant contribution. It quickly raises T_e, which slows recombination and leads
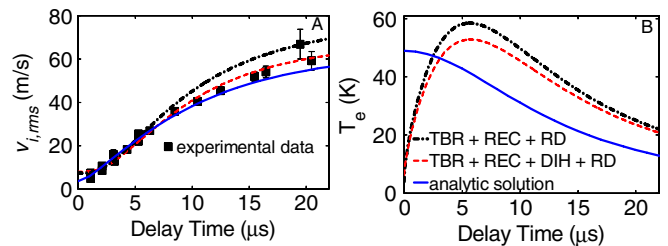

FIG. 3 (color online).   (a) Ion velocity and (b) electron temperature for $\Gamma_e \sim 1$ [$2E_e/3k_B = 4$ K, $n_0(0) = 8 \times 10^{15}$ cm^{-3}, $\sigma(0) = 1.0$ mm]. (a) The numerical simulation including all heating effects matches the data with no adjustable parameters. For this relatively high density, the initial heating from DIH slows TBR and REC enough to produce an observable effect. The analytic solution fit is poor, but yields $T_e(0) = 49 \pm 2$ K. (b) The electron temperature shows drastic heating at early times and $T_e(0)$ no longer provides a good estimate of $T_{e,\text{max}}$.
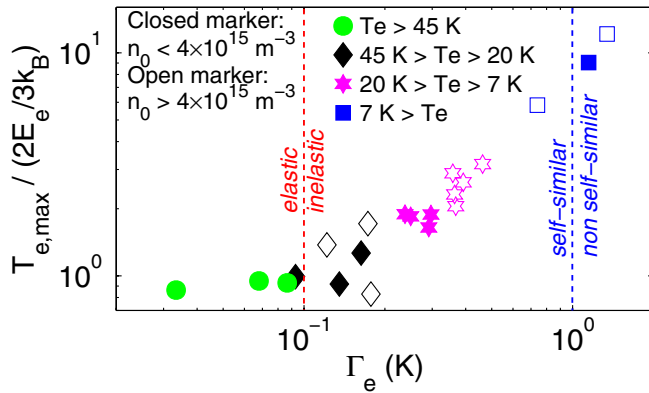
FIG. 4 (color online). Electron heating summary. The plasma dynamics are parametrized well by $\Gamma_e(n_0, E_e)$. $T_{e,\max}$ is the maximum electron temperature attained during the evolution. The heating is negligible in the elastic-collisional regime ($\Gamma_e <$ 0.1 [18]), and $T_{e,\max}/(2E_e/3k_B) \approx 1$. In the inelastic collisional regime, the heating becomes significant and increases with increasing density and decreasing $2E_e/3k_B$. Beyond $\Gamma_e \approx 1$, the expansion ceases to be self-similar.

to a lower $T_{e,\max} = 53$ K. The agreement between data and simulation indicates no significant deviation from classical TBR theory [4].

Figure 4 summarizes our results for electron heating in UNPs. The data are organized according to initial Γ_e [18], and it displays a clear trend in the heating of the electrons as previously observed in [8,11]. The onset of heating occurs at the crossover between the inelastic and elastic-collisional regime. For initial $\Gamma_e \gtrsim 1$, the expansion ceases to be self-similar.

We have described the use of spectroscopic ion-velocity measurements and numerical simulations as a time-resolved probe of electron dynamics in UNPs. It resolves outstanding questions regarding evolution of electron temperature and shows that dynamics vary greatly for different initial electron kinetic energy and plasma density. This work identifies the relative contributions and time scales of various processes, demonstrates the importance of radiative decay and disorder-induced electron heating for the first time in UNPs, and shows no deviations from traditional, classical TBR theories.

[1] T. C. Killian, Science **316**, 705 (2007).

[2] T. C. Killian, T. Pattard, T. Pohl, and J. M. Rost, Phys. Rep. (to be published).

[3] S. G. Kuzmin and T. M. O'Neil, Phys. Plasmas **9**, 3743 (2002).

[4] P. Mansbach and J. Keck, Phys. Rev. **181**, 275 (1969).

[5] T. C. Killian *et al.*, Phys. Rev. Lett. **86**, 3759 (2001).

[6] F. Robicheaux and J. D. Hanson, Phys. Plasmas **10**, 2217 (2003).

[7] T. Pohl, T. Pattard, and J. M. Rost, Phys. Rev. A **70**, 033416 (2004).

[8] S. Kulin, T. C. Killian, S. D. Bergeson, and S. L. Rolston, Phys. Rev. Lett. **85**, 318 (2000).

[9] J. L. Roberts, C. D. Fertig, M. J. Lim, and S. L. Rolston, Phys. Rev. Lett. **92**, 253003 (2004).

[10] E. A. Cummings, J. E. Daily, D. S. Durfee, and S. D. Bergeson, Phys. Rev. Lett. **95**, 235001 (2005).

[11] E. A. Cummings, J. E. Daily, D. S. Durfee, and S. D. Bergeson, Phys. Plasmas **12**, 123501 (2005).

[12] R. S. Fletcher, X. L. Zhang, and S. L. Rolston, Phys. Rev. Lett. **96**, 105003 (2006).

[13] A. N. Tkachev and S. I. Yakovlenko, Quantum Electron. **30**, 1077 (2000).

[14] S. Mazevet, L. A. Collins, and J. D. Kress, Phys. Rev. Lett. **88**, 055001 (2002).

[15] C. E. Simien *et al.*, Phys. Rev. Lett. **92**, 143001 (2004).

[16] S. B. Nagel *et al.*, Phys. Rev. A **67**, 011401 (2003).

[17] M. S. Murillo, Phys. Rev. Lett. **87**, 115003 (2001).

[18] For characterizing dynamics according to initial conditions, Γ_e is calculated using initial peak density and the naïve assumption of initial $T_e = 2E_e/3k_B$. The plasma may be far from thermal equilibrium at these early times.

[19] S. D. Bergeson and R. L. Spencer, Phys. Rev. E **67**, 026414 (2003).

[20] D. S. Dorozhkina and V. E. Semenov, Phys. Rev. Lett. **81**, 2691 (1998).

[21] T. Pohl, T. Pattard, and J. M. Rost, Phys. Rev. Lett. **92**, 155003 (2004).

[22] A. V. Baitin and K. M. Kuzanyan, J. Plasma Phys. **59**, 83 (1998).

[23] V. F. Kovalev and V. Y. Bychenkov, Phys. Rev. Lett. **90**, 185004 (2003).

[24] S. Laha, P. Gupta, H. Gao, C. E. Simien, J. Castro, and T. C. Killian (to be published).

[25] Threshold lowering is sometimes also considered, but electron DIH includes this effect because it is related to spatial correlations between particles.

[26] T. Pohl, T. Pattard, and J. Rost, J. Phys. B **38**, S343 (2005).

[27] H. A. Bethe and E. E. Salpeter, *Quantum Mechanics of One- and Two-Electron Atoms* (Plenum, New York, 1977).

[28] Y. Hahn, Phys. Lett. A **231**, 82 (1997).

[29] Y. Hahn, Phys. Lett. A **264**, 465 (2000).

[30] S. A. Maiorov, A. N. Tkachev, and S. I. Yakovlenko, Phys. Scr. **51**, 498 (1995).